

Article

Improvements to and Experimental Validation of PI Controllers Using a Reference Bias Control Algorithm for Wind Turbines

Taesu Jeon ¹, Dongmyoung Kim ¹ and Insu Paek ^{1,2,*}

¹ Department of Integrated Energy & Infra System, Kangwon National University, Chuncheon-si 24341, Gangwon, Korea

² Department of Mechatronics Engineering, Kangwon National University, Chuncheon-si 24341, Gangwon, Korea

* Correspondence: paek@kangwon.ac.kr; Tel.: +82-033-250-6379

Abstract: In this study, a reference bias control (RBC) algorithm for variable speed and variable pitch wind turbines was designed and validated. To improve the performance of conventional PI control algorithms, the RBC algorithm applies biased references to power and pitch angle to the pitch and the torque control loops, respectively. To validate the control performance of the improved RBC algorithm, hardware in the loop simulator (HILS) was conducted using a commercial programmable logic controller (PLC). The performance of a conventional PI control algorithm and the proposed RBC algorithm were compared for the target wind turbine model in terms of both the transition region and the rated power region. In the transition region, the proposed RBC algorithm improved the sudden dips in the generator torque and power, which often occur when using a control algorithm with a switching logic. As a result, the damage equivalent load (DEL) of the main shaft was reduced by 15%. In the rated power region, the rotor speed deviation was reduced by 22% and the power deviation was reduced by 21%. To experimentally validate the control performance and applicability of the RBC algorithm, wind tunnel testing using a wind turbine scaled model was additionally performed. Similarly to the HILS testing result, it was confirmed that the DEL of the main shaft and fluctuation of the rotor speed and power decreased with the proposed RBC algorithm.

Keywords: proportional–integral (PI) control; switching logic; reference bias control (RBC); hardware in the loop simulator (HILS); wind tunnel testing



Citation: Jeon, T.; Kim, D.; Paek, I. Improvements to and Experimental Validation of PI Controllers Using a Reference Bias Control Algorithm for Wind Turbines. *Energies* **2022**, *15*, 8298. <https://doi.org/10.3390/en15218298>

Academic Editor: Taimoor Asim

Received: 27 September 2022

Accepted: 25 October 2022

Published: 7 November 2022

Publisher's Note: MDPI stays neutral with regard to jurisdictional claims in published maps and institutional affiliations.



Copyright: © 2022 by the authors. Licensee MDPI, Basel, Switzerland. This article is an open access article distributed under the terms and conditions of the Creative Commons Attribution (CC BY) license (<https://creativecommons.org/licenses/by/4.0/>).

1. Introduction

Modern wind turbines have been developed to be variable speed and variable pitch (VSVP) models that can control their generator reaction torque and blade pitch angle to increase or decrease the efficiency of their power production, depending on the operating region. The basic structure of the control algorithm for VSVP wind turbines consists of a classical control-based torque control loop and a pitch control loop. A method for using a switching logic has been proposed and applied to different control strategies, according to the operating region [1].

In the maximum power region, where the wind speed is lower than the rated value, while the pitch control loop keeps the blade pitch angle at a fine pitch angle, the torque control loop uses either a generator speed–torque look-up table or a proportional–integral (PI) or proportional–integral–differential (PID) control algorithm to track the maximum power point. In the rated power region, where the wind speed is higher than the rated value, the pitch control loop performs blade pitch PI or PID control to maintain the generator speed of the wind turbine at the rated value. At the same time, the torque control loop performs generator reaction torque control to keep the generator torque at the rated value or to maintain the generator power at the rated value. In addition, algorithms for the smooth connection between two control regions are applied in transition regions in which wind speed is a rated value [2,3].

Controllers that have been designed based on these strategies can serve as baseline power controllers but cannot reflect both the efficiency of power production and the structural stability. Therefore, studies have been conducted to improve the power performance and load reduction performance of baseline control algorithms. To improve the power performance of baseline controllers, gain scheduling techniques have been applied to pitch PI control algorithms to maintain a uniform sensitivity to changes in wind speed [4]. In addition, in order to reduce fluctuations in rotor speed and generator power, a study was conducted to calculate the changes in pitch angle according to changes in wind speed in advance and then add it to the pitch command [5]. To improve the load reduction performance of baseline controllers, studies have been conducted to apply drivetrain damper, peak shaving and tower damper techniques to conventional classical control techniques to reduce fatigue loads in the drivetrains, blades and towers of wind turbines [6–8]. In these studies, drivetrain dampers were able to reduce the in-plane load of blades by 27.0% and the side–side load of towers by 57.0%, while the peak shaving technique reduced the out-of-plane load of blades by 14.0% and the fore–aft load of towers by 9.4%. In addition, fatigue loads in towers and blades could be significantly reduced using the tower damper and individual pitch control techniques.

However, because there are limits to the structures of conventional single-input single-output (SISO) PI control algorithms, studies have been conducted on modern control algorithms using new structures that can regulate various control variables, such as generator speed, power and tower vibration, in order to comprehensively consider all performance conditions. Linear quadratic regulator (LQR) control algorithms that minimize quadratic cost functions to obtain optimal solutions have been able to reduce deviations in generator speed by 46.2% and the fore–aft load of towers by 20.1% [9]. In addition, LQR controllers based on fuzzy logic (LQRF) algorithms that considered the nonlinear effects of wind turbines have reduced power fluctuations by up to 38.9% and tower vibrations by 12.4% [10,11]. Moreover, model predictive control (MPC) algorithms that calculate the optimal state of predicted models, along with control variable constraints, have improved power quality, despite the 50% uncertainty that is caused by inductance [12]. The H_∞ control algorithm, which achieves a robust performance by evaluating transfer functions for uncertain systems, has shown through dynamic simulations that tower loads could be reduced by up to 7.8% and blade loads could be reduced by up to 26.3% compared with baseline PI control algorithms [13].

Although the modern control algorithms that have been proposed in previous studies have shown superior performance compared with conventional control algorithms, they are not easy to replace the conventional PI control algorithms because the performance and stability of the conventional algorithms have been validated over long periods of time. In order to apply new control algorithms to wind turbines, the performance of the controllers must be validated experimentally through field tests. However, long-term validation using large wind turbines that have already been commercialized is not easy in reality due to the costs and the problems concerning compatibility with conventional algorithms. Therefore, methods are being considered that simply tune the control gain without significantly changing the structure of conventional wind turbine algorithms or add additional control loops with specific control purposes to the torque or pitch command independently.

Classical control-based wind turbine control algorithms perform torque and pitch control depending on the measured generator speed and switch between pitch and torque control strategies in transition regions using a switching logic. The switching logic only determines the operating points of wind turbines and transmits this information to the pitch and torque control loops, but its form varies depending on the implementation method. Bossanyi et al. proposed a switching logic that allowed only one control loop to be activated at a time [2]. Nam et al. implemented the method that was proposed in [2] using SR flip-flop logic [3]. Ruz et al. proposed a switching logic that used interpolation functions to reduce the unwanted transience in the transition control region [14].

However, a switching logic can often cause the following problems. When a switching logic fails to properly switch both the torque and pitch control algorithms in transition regions, a control algorithm is always performed to track the set point of the generator speed without the region in which the blade pitch angle is maintained at a fine pitch angle, resulting in increased fatigue load accumulation and reduced power performance [15]. Pao et al. showed that structural damage could be caused by extreme loads and fatigue loads when a proper switching logic was not applied in turbines on which actual field tests had been conducted [16]. In addition, a switching logic that has been in some previous studies had the problem of sudden dips in transition regions [5,17]. In a study by Kim et al., sudden dips that were generated by the switching logic in the transition regions were mentioned, but this was only used to compare control performances. However, no improvements have been proposed in the literature that could help conventional PI control algorithms to avoid generating these sudden dips [17].

Previous studies have informed two important requirements for improving conventional PI control algorithms. Firstly, torque and pitch control algorithms are required that do not depend solely on measured generator speed. Secondly, there is a need for algorithms that can apply control strategies simultaneously, without the occurrence of transient responses in transition regions. Additionally, for easy application to modern wind turbines, sufficient control performance, reliability and applicability must be ensured without significantly changing the structure of conventional PI control algorithms.

These requirements could be satisfied using bias control algorithms. Deflection in a control loop is an algorithm that adds or subtracts certain actions by applying filters or gains to measurable signals or errors in signals. Therefore, it is possible to consider other states, such as generator power and pitch angle, in addition to the variables that need to be controlled without significantly changing the structure of conventional PI control algorithms. In addition, even without a specific switching logic, transient responses that arise from transitions between control strategies could be smoothed using the filters and gains of bias terms with limiters [18].

This study was not the first time that bias control without switching logic has been applied to wind turbine control systems. Studies have been conducted on constrained reference power control algorithms that use set-point control [19]. In this study, a controller was designed that was capable of automatically de-rating a power command when the operating conditions of the wind turbine became unstable due to gusts of wind and it was validated through dynamic simulations. Through the simulations, it was shown that the proposed controller could increase power generation by 2.45%. However, even though the bias control algorithm was applied without switching logic, a comparative analysis of a PI control algorithm that used a conventional switching logic was not performed in transition regions and sufficient analysis of the advantages of using a conventional switching logic was not performed. In addition, no experimental validation studies, such as hardware in the loop simulator (HILS) and wind tunnel testing, were performed to validate the proposed algorithms.

Therefore, in this study, to mitigate the problems that arise from the switching logic in conventional PI control algorithms, we designed a reference bias control (RBC) algorithm for an NREL 5MW wind turbine and validated its improved control performance. The RBC PI control algorithm that is proposed in this paper was experimentally validated through HILS using a commercial PLC and wind tunnel testing using a scaled wind turbine model to validate its improved control performance compared with a PI control algorithm that used a conventional switching logic.

2. Target Wind Turbine Model

The target wind turbine model of this study was the NREL 5MW reference wind turbine [20]. This type of wind turbine was numerically modeled on DNV-Bladed (4.12, DNV, Oslo and Norway) to perform real-time hardware in the loop simulations with the proposed controller. The rated power of the target wind turbine model is 5 MW and it has a rotor

diameter of 126 m and a hub height of 90 m. The target wind turbine that was numerically modeled in Bladed is shown in Figure 1 and brief specifications are presented in Table 1.

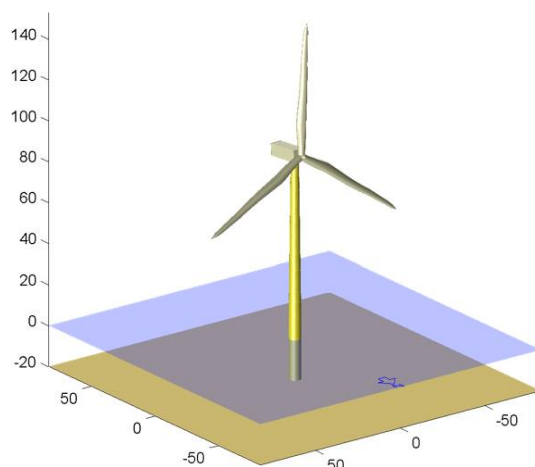


Figure 1. Model of NREL 5MW wind turbine.

Table 1. Specifications of NREL 5MW wind turbines.

Parameter	Unit	Value
Rating	MW	5
Rated Rotor Speed	rpm	12.1
Rated Generator Torque	kNm	43.1
Gear Ratio	-	97
Wind Turbine Site Class	-	Class 1A
Rotor Diameter	m	126
Hub Height	m	90
Cut-in/Rated/Cut-out Wind Speed	m/s	3/11.4/25

3. Controller Design

3.1. Reference Bias Control Algorithm

The pitch control loop and torque control loop that control wind turbines receive generator speed signals and perform feedback control to reach the reference generator speed. In this study, the RBC algorithm offered a method of calculating new reference generator speeds by applying the bias that was calculated by the feedback loop of the generator power and pitch angle in the pitch and torque control loop, respectively. Equation (1) represents the reference generator speed that was used to calculate the target value of the generator speed.

$$\Omega_{g,ref,dppt} = \min(\Omega_{g,rated}, (P_{cmd}/k_{g,opt})^{\frac{1}{3}}) \quad (1)$$

The goal of speed control for wind turbines that are located in regions where the wind speed is higher than the rated value is basically to maintain the rated generator speed. However, when the power of wind turbines needs to be limited to a specific level, the reference value of the generator speed may vary depending on the required power. In this study, the function of the demanded power point tracking (DPPT) was implemented using the optimal mode gain $k_{g,opt}$. When the minimum value of the rated generator speed $\Omega_{g,rated}$ and the generator speed for tracking the required power P_{cmd} are calculated, the rated generator speed and the generator speed that produces the required power can be simultaneously regulated.

In a pitch control loop, the bias term for the power is calculated from power feedback to prevent pitch control from being performed in the maximum power region and to reduce deviations in the power. The bias term for the reference generator speed in a torque control loop is calculated from pitch angle feedback to reduce the mutual interference effects of

pitch control in transition regions and to prevent frequent torque command changes in the rated power region. The bias terms for the reference generator speed of a pitch control loop and a torque control loop are described in Equations (2) and (3), respectively:

$$\delta\zeta_{\beta} = LPF \left\{ gain_{P_{to}\Omega} \left(P_{mea} - \min(P_{rated}, P_{cmd}) \right) \right\} \tag{2}$$

$$\delta\zeta_{\tau} = LPF \left\{ gain_{\beta_{to}\Omega} \left(\beta_{mea} - \beta_{fine} \right) \right\} \tag{3}$$

The calculation of bias terms is achieved by applying gains and low pass filters to the errors in measured signals (P_{mea} and β_{mea}). Bias gains ($gain_{P_{to}\Omega}$ and $gain_{\beta_{to}\Omega}$) are determined by the scaling values of signals with different dimensions and the bias weight. A low pass filter (LPF) is applied to remove noise and unnecessary vibration components that are mixed into bias terms. The reference generator speed $\bar{\Omega}_{g,ref}$ is then calculated using the bias terms $\delta\zeta$ and can be expressed as:

$$\bar{\Omega}_{g,ref} = \Omega_{g,ref,dppt} - \delta\zeta \tag{4}$$

Figure 2 shows the RBC algorithm in Equation (4) as a block diagram. As shown in Figure 2a, a reference value was calculated for the generator speed in the pitch control loop. The pitch loop bias $\delta\zeta_{\beta}$ with respect to an error between the reference power and the measured power P_{mea} was subtracted from the reference generator speed in the pitch control loop. As for the reference power, the minimum values of the rated power P_{rated} and the power were applied in consideration of the demanded power P_{cmd} . In Figure 2b, a reference value was calculated for the generator speed in the torque control loop. The torque loop bias $\delta\zeta_{\tau}$ with respect to an error in the fine pitch angle β_{fine} and the measured pitch angle β_{mea} was subtracted from the reference generator speed in the torque control loop.

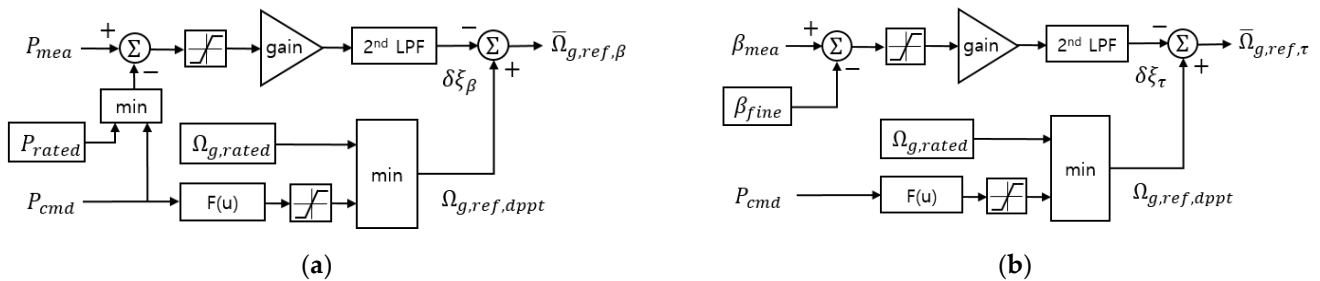


Figure 2. Block diagrams of RBC algorithms: (a) Pitch control loop; (b) Torque control loop.

3.2. MPPT Control with a Torque Limiter

Maximum power point tracking (MPPT) control is a strategy to control generator reaction torque so that wind turbines can track the max Cp line for each operating region when they are located in regions where the wind speed is lower than the rated value [1]. The simplest torque control method for implementing this strategy is the application of a reaction torque command that is relative to the generator speed using a two-dimensional (2D) look-up table. Torque scheduling uses look-up tables to smooth torque set-points by applying appropriate slopes or smoothing functions to the torque set-points at the minimum rotor speed and the rated speed [2,3]. However, in this case, since the smoothed portion of the max Cp line deviated from the line, there was a slight loss in terms of power production efficiency. Therefore, in this study, a torque PI control algorithm with torque limiters was used to design the controller so that the target wind turbine model could track the max Cp line as much as possible.

Figure 3 shows the generator speed and torque trajectory that were required for the target wind turbine model to perform MPPT control with the torque limiter. Figure 3a shows the aerodynamic torque, max Cp line, rated power curve and torque trajectory by wind speed and generator speed. In addition to the max Cp lines, the torque trajectory

included regions that were separated from the max Cp line due to the limitations of the minimum start-up generator speed of the wind turbine and the rated generator speed for achieving the rated conditions. The generator reaction torque limiter that was used to implement the nonlinear trajectory is shown in Figure 3b. The torque limiter consisted of an upper and lower limit, including the max Cp line. The MPPT control was performed along the max Cp line trajectory with the same upper and lower limits. The PI control of the generator reaction torque was performed in regions with generator speed limitations to regulate the reference generator speed.

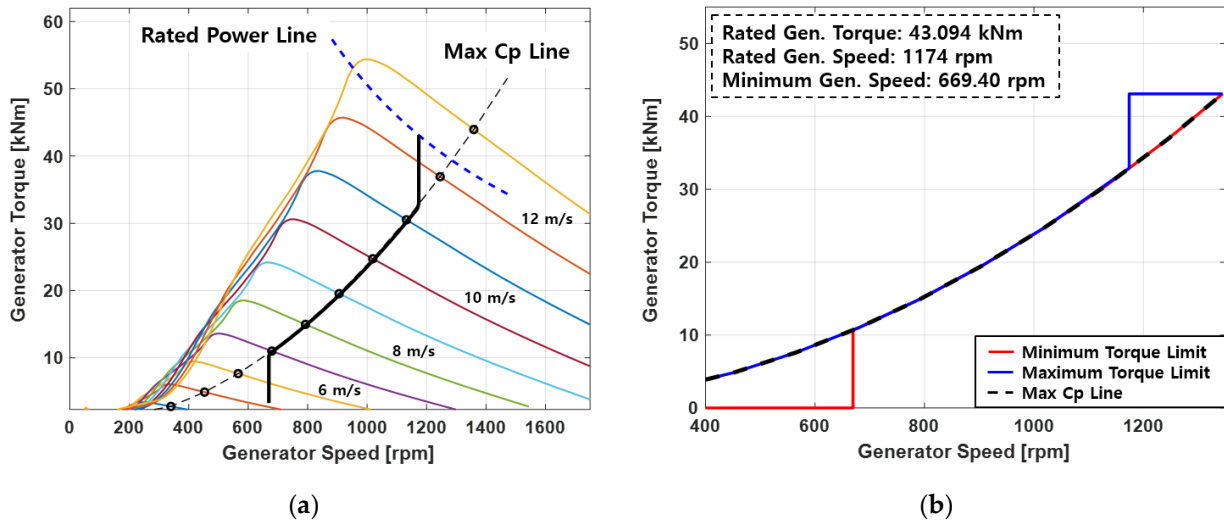


Figure 3. Strategy of MPPT control: (a) set-point of generator reaction torque; (b) generator reaction torque limiters.

To apply the upper and lower limits of the generator reaction torque in the torque control loop, an algorithm was required to calculate the upper and lower limits. Equation (5) was used as the reference torque to obtain the trajectory of the upper torque limit. The reference torque considering the demanded power was calculated using the minimum value of the rated generator torque $\tau_{g,rated}$ and torque capable of producing the demanded power.

$$\tau_{g,ref,dppt} = \min(\tau_{g,rated}, (P_{cmd}) / (k_{g,opt})^{\frac{1}{3}}) \tag{5}$$

Equation (6) represents the upper torque limit $\tau_{UL,dppt}$ considering the demanded power. Using Equation (6), MPPT control was performed when the measured generator speed $\Omega_{g,mea}$ was lower than the rated generator speed and the reference torque considering the demanded power was maintained when the measured generator speed was higher than the rated generator speed.

$$\tau_{UL,dppt} = \begin{cases} \tau_{g,ref,dppt} & \text{if } \Omega_{g,mea} \geq \Omega_{g,rated} \\ k_{g,opt}\Omega_{g,mea}^2 & \text{otherwise} \end{cases} \tag{6}$$

Using Equation (7), the lower torque limit was used to minimize the torque command when the measured generator speed was lower than the minimum generator speed $\Omega_{g,min}$ for the start-up of the wind turbine and MPPT control was performed when the measured generator speed was higher than the rated generator speed.

$$\tau_{LL} = \begin{cases} 0 & \text{if } \Omega_{g,mea} \leq \Omega_{g,min} \\ k_{g,opt}\Omega_{g,mea}^2 & \text{otherwise} \end{cases} \tag{7}$$

However, when the demanded power was input into the controller, the upper torque limit could be smaller than the max Cp line, so the lower torque limit $\tau_{LL,dppt}$ considering

the demanded power was calculated using the minimum values of the upper and lower torque limits, as shown in Equation (8):

$$\tau_{LL,dppt} = \min(\tau_{UL,dppt}, \tau_{LL}) \tag{8}$$

3.3. PI Control Algorithm

In this study, a PI control algorithm was applied as a control algorithm to regulate the generator speed so that the performances of the controllers could be compared. Equation (9) was used to describe the PI control algorithm:

$$u(t) = K_p(\Omega_{g,mea} - \bar{\Omega}_{g,ref}) + K_i \int (\Omega_{g,mea} - \bar{\Omega}_{g,ref}) dt \tag{9}$$

The control input u was calculated by applying the proportional gain K_p and integral gain K_i to the difference between the reference generator speed that was calculated by the RBC algorithm and the measured generator speed. Figure 4 shows an overall block diagram of the PI control algorithm with the RBC algorithm. The structure of the baseline PI control algorithm to be compared with the RBC PI control algorithm is a form in which the RBC is not applied in the block diagram of Figure 4 and the switch logic with set-reset (SR) flip-flop logic is applied [17].

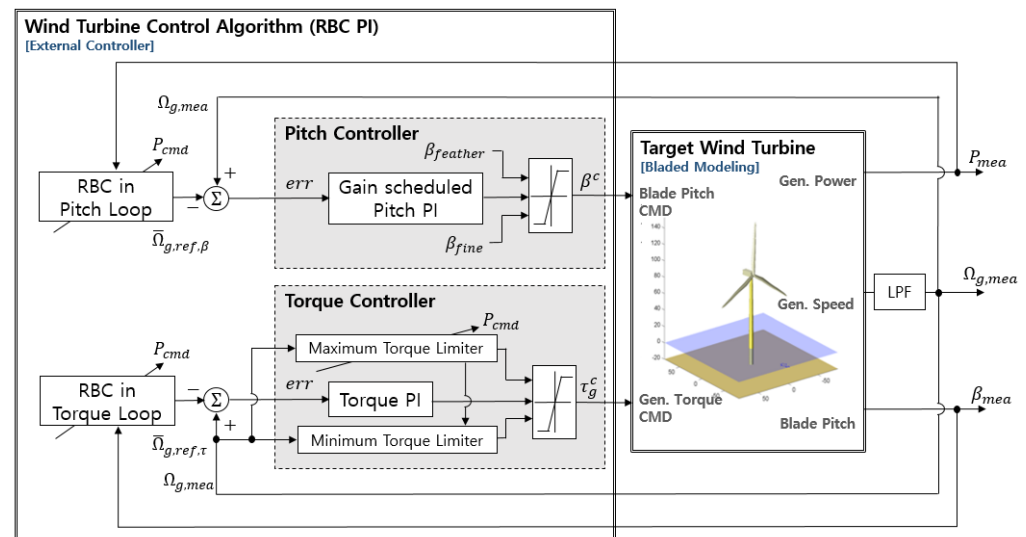


Figure 4. Block diagram of RBC PI control algorithm.

4. Controller Validation

4.1. Hardware in the Loop Simulator

To validate the performance of the proposed control algorithm, the experiment using hardware in the loop simulator (HILS) was performed using commercial Bachmann-PLC and DNV-Bladed programs. HILS offer an intermediate validation step that lies between simulation validation and experimental validation. The control performance and applicability of controllers can be validated by uploading control algorithms that were designed on real commercial PLC programs. Figure 5 shows a flowchart of HILS.

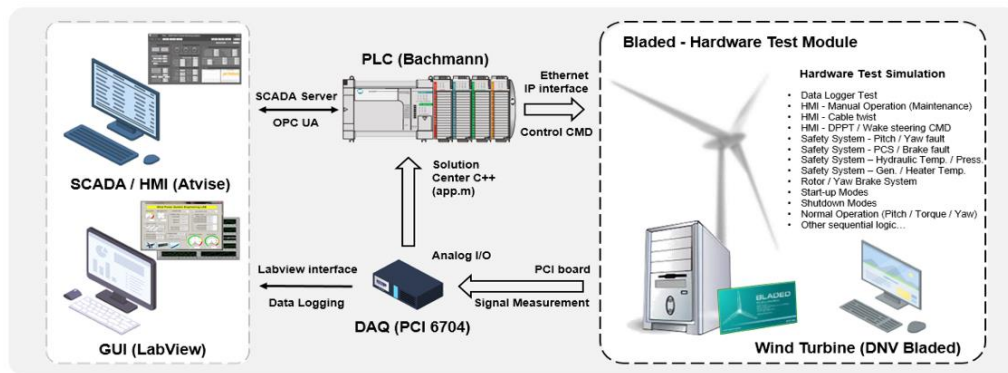


Figure 5. Flowchart of hardware in the loop simulator.

The proposed control algorithm was designed in MATLAB/Simulink (R2019b, The MathWorks, Inc., Natick, MA, USA) and compiled into a C file and uploaded to a PLC. In order to interface the Bachmann PLC with the uploaded controller implements to the target wind turbine model and operator, a supervisory control and data acquisition (SCADA), human-machine interface (HMI) and graphical user interface (GUI) were implemented using Atvise (Atvise 3.5, Bachmann Electronic GmbH, Feldkirch, Austria) and LabVIEW (LabVIEW2020, National Instruments Corporation, Austin, TX, USA). A PC that ran the hardware test module of the Bladed program imitated the dynamics of the numerically modeled target wind turbine. The PC-modeled turbine, controller-uploaded PLC and data acquisition (DAQ/PCI-6704) formed a hardware loop that could perform real-time hardware testing [21].

In this study, the experiment using HILS was performed under normal turbulence model (NTM) wind conditions to international electrotechnical commission (IEC) standards in order to validate the performance, reliability and applicability of the proposed controller in a control system environment using an actual commercial PLC [22]. Figure 6 shows the configuration of the real-time HILS.



Figure 6. HILS environment on LAB scale.

The normal operation of NREL 5MW wind turbines was simulated for 200 s under the conditions of average wind speeds of 13 m/s and 18 m/s, respectively, which are the transition and rated power regions. As the controller controlled the target wind turbine, a baseline PI control algorithm using a mode switch and the RBC PI control algorithm using the RBC algorithm that is proposed in this paper were applied. The simulation results were compared and analyzed to evaluate the performances of the two control algorithms.

Figure 7 shows the HILS testing results from the baseline PI control algorithm and the RBC PI control algorithm for the model NREL 5MW wind turbine. In order to compare and analyze the control performance of each control algorithm, the wind speed, rotor

speed, blade pitch angle, generator torque and generator power were measured and are shown in Figure 7. Figure 7a shows the simulation results in the transition regions under the conditions of an average wind speed of 13 m/s and a turbulence intensity of 19%. In Figure 7a, the control operations of the baseline PI control algorithm and RBC PI control algorithm in the transition region can be confirmed around 50 s and 140 s. From the HILS testing results of the baseline PI control algorithm, it was possible to confirm a sudden dip that sometimes occurs when switching logic is used in the generator torque and generator power. On the other hand, the RBC PI control algorithm biased the reference generator speed of the pitch and torque control loops using power and pitch angle errors, respectively. Then, the RBC PI control algorithm slowly reduced torque before the baseline PI control algorithm, around 50 s and 140 s, and used pitch angles around 80 s and 145 s before the baseline PI control algorithm. As a result, the RBC PI control algorithm reduced the torsional load of the main shaft and deviations in the rotor speed. Figure 7b shows the simulation results in the rated power region under the conditions of an average wind speed of 18 m/s and a turbulence intensity of 17%. In Figure 7b, it can be seen that the baseline PI control algorithm and the RBC PI control algorithm both maintained the rated torque and performed pitch control. However, in the RBC PI control algorithm, the deviations in rotor speed and generator power were reduced because the reference generator speed was biased using power feedback.

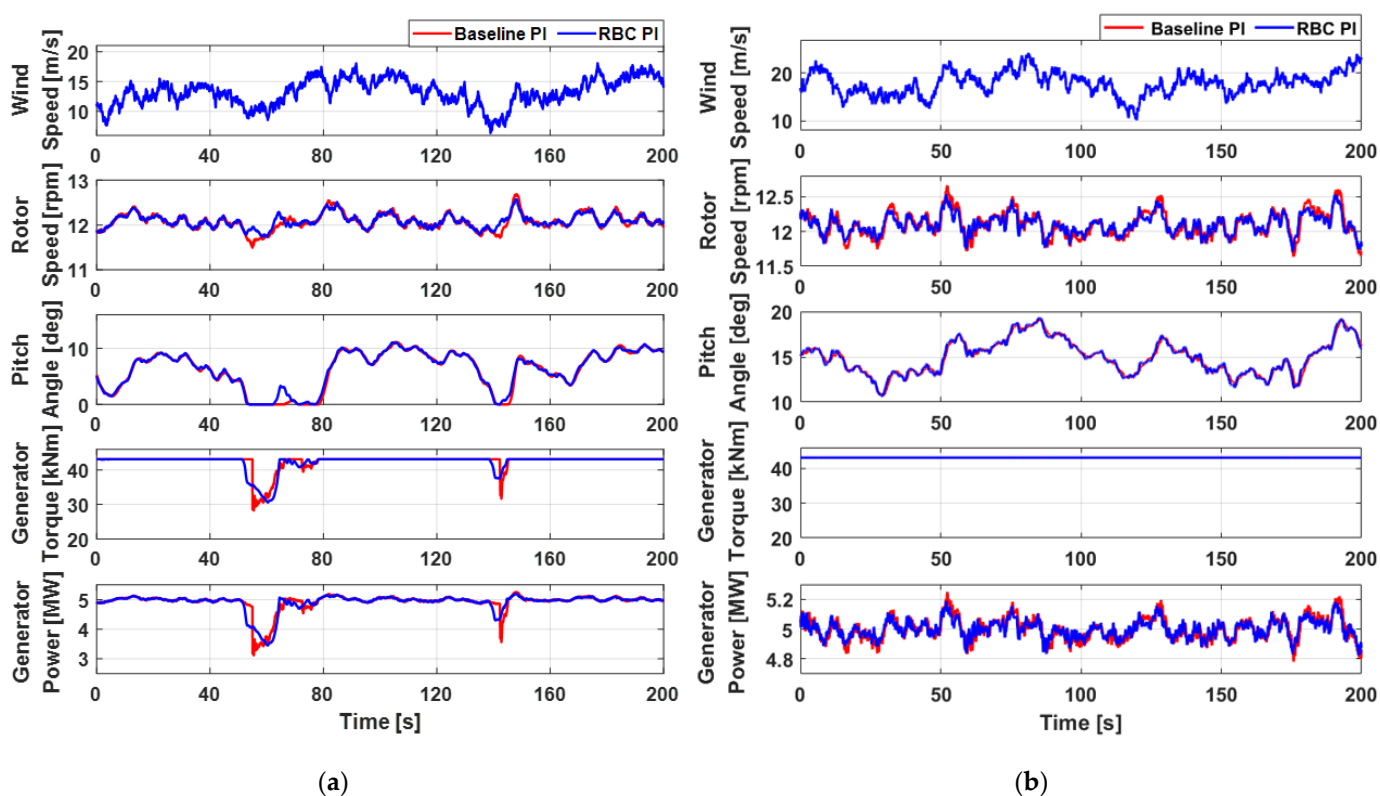


Figure 7. Results from HILS testing of NREL 5MW wind turbine: (a) average wind speed of 13 m/s and 19% turbulence intensity; (b) average wind speed of 18 m/s and 17% turbulence intensity.

The results from the quantitative comparison of the simulations for the target wind turbine are shown in Table 2. The evaluation metrics of the control performance of the control algorithms were the mean and standard deviation of rotor speed and generator power and the damage equivalent load (DEL) of the torsional load of the main shaft. These metrics were selected because in order to check whether the model wind turbine could perform stable control, it was necessary to check the rotor speed, which was the variable to be controlled, and the state of the generator power. The DEL of the torsional load of the main shaft was used to evaluate the transient responsiveness of the torque control.

As a result, in the transition regions, the RBC PI control algorithm reduced the standard deviation of the rotor speed and generator power by 19.72% and 2.86%, respectively, compared with the baseline PI control algorithm. In addition, the DEL of the torsional load was reduced by 14.74% due to the improvement in the sudden dips. In the rated power region, the RBC PI control algorithm reduced the standard deviation of the rotor speed and generator power by 22.40% and 21.35%, respectively, compared with the baseline PI control algorithm, without changing the mean of the rotor speed and generator power.

Table 2. Quantitative comparison of control performance for NREL 5MW wind turbine during HILS testing.

Operating Region	Hardware in the Loop Simulator	Control Performance for NREL 5MW Wind Turbine				
		Mean		Std. Dev.		DEL
		Ω_r (rpm)	P (MW)	Ω_r (rpm)	P (MW)	T (MNm)
Transition Region	Baseline PI (A)	12.080	4.923	0.180	0.300	0.893
	RBC PI (B)	12.091	4.915	0.144	0.291	0.762
	(B-A)/A (%)	0.094	−0.168	−19.716	−2.861	−14.737
Rated Power Region	Baseline PI (C)	12.103	5.001	0.181	0.076	1.344
	RBC PI (D)	12.101	5.003	0.140	0.060	1.312
	(D-C)/C (%)	−0.021	0.030	−22.402	−21.351	−2.342

4.2. Wind Tunnel Testing

The control performance, reliability and applicability of the RBC PI control algorithm that is proposed in this paper were experimentally validated through wind tunnel testing at a large wind tunnel test site (Jeolla-do, Korea), as well as the HILS testing. The large wind tunnel test site is a two-story building with an internal circulation structure for the wind. This site consists of a high-speed test section and a low-speed test section, a corner vane and a fan motor. The wind tunnel has the dimensions of $40 \times 12 \times 2.5$ m. Therefore, a scaled wind turbine model that was capable of validating the control algorithm was used for the wind tunnel testing.

The scaled wind turbine model had a rated power of 39.7 W, a rated rotor speed of 678 rpm, a rotor diameter of 1.1 m and a hub height of 0.9 m. The scaled wind turbine model was originally designed and developed by researchers from the Munich Institute of Technology to validate controllers for large wind turbines [23]. However, for this study, the scaled wind turbine model was modified using 3D-printed blades and new control algorithms. The scaled wind turbine model was operated and monitored via connections to a PC in the control room using the PLC that had been validated for the control system through the HILS testing.

The wind tunnel testing environment and the scaled wind turbine model that was used for the experiments are shown in Figure 8. Figure 8a shows the overall wind tunnel setup. The wind tunnel testing experiments in this study were conducted in the low-speed test section. The wind was formed by the fan motor on the second floor and was transmitted to the low-speed test section on the first floor by the corner van. Figure 8b shows the low-speed test section where the wind tunnel testing was performed. A 10% turbulence intensity was implemented using wedges at the wind input. Inside the wind tunnel, the scaled wind turbine model, a PLC cabinet and an anemometer were installed for the experiments. Figure 8c shows the scaled VSVP-type horizontal wind turbine model that was capable of pitch control and torque control.

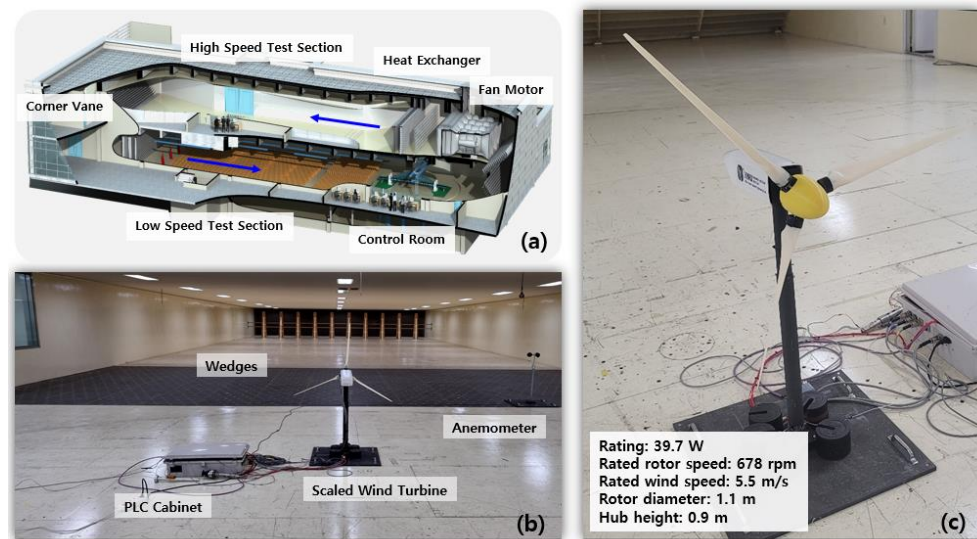


Figure 8. Wind tunnel testing environment: (a) overall wind tunnel setup; (b) low-speed test section; (c) scaled wind turbine model that was capable of pitch control and torque control.

The wind tunnel testing of the scaled wind turbine model was conducted for 60 s under the conditions of average wind speeds of 5.8 m/s and 8.1 m/s, respectively, which are the transition and rated power regions. A 10% turbulence intensity was also implemented using wedges at the wind input. The baseline PI control algorithm and the RBC PI control algorithm were designed and applied to the PLC to control the scaled wind turbine model in the same way as they would be applied in an NREL 5MW wind turbine.

Figure 9 shows the results from the wind tunnel testing of the baseline PI control algorithm and RBC PI control algorithm for the scaled wind turbine model. Figure 9a shows the results from the wind tunnel testing on the transition regions, with an average wind speed of 5.8 m/s and a turbulent intensity of 10%. In Figure 9a, the transient responses in the transition regions can be seen. In the baseline PI experiment, it was confirmed around 21 s, 30 s and 35 s. In the RBC PI experiment, it was confirmed around 23 s, 28 s and 42 s. As shown in Figure 7a, the results from the HILS testing of the NREL 5MW wind turbine showed that the RBC PI control algorithm responded appropriately to the transient responses in the transition regions using torque and pitch with biased information about the reference generator speed. These operations were also confirmed to be around 50 s, as shown in Figure 7a. Figure 9b shows the results from the wind tunnel testing on the rated power region, with an average wind speed of 8.1 m/s and a turbulence intensity of 10%. Figure 9b shows that the baseline PI control algorithm and the RBC PI control algorithm performed pitch control to regulate the generator speed while maintaining the rated torque. Unlike HILS, wind tunnel experiments cannot reproduce the same wind in time series, so wind conditions were different, but the average wind speed and turbulence intensity were tried to be close. In addition, although the simulation generated turbulence intensity calculated by NTM according to the average wind speed, it is very difficult to implement specific turbulence intensity in wind tunnel experiments. Therefore, the maximum turbulence intensity (approximately 10%) that can be implemented in all wind tunnel experiments was applied.

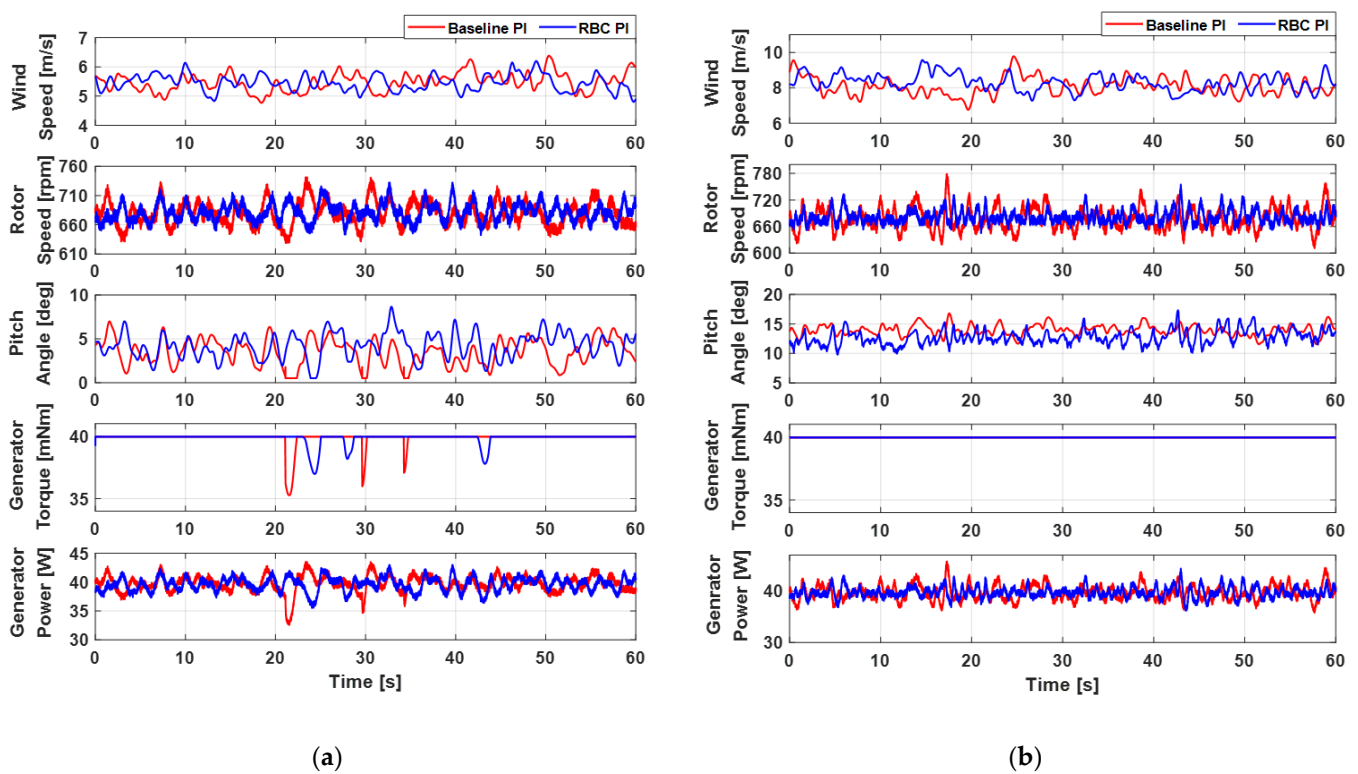


Figure 9. Results from wind tunnel testing of scaled wind turbine model: (a) average wind speed of 5.8 m/s and 10% turbulence intensity; (b) average wind speed of 8.1 m/s and 10% turbulence intensity.

The results from the quantitative comparison of the wind tunnel testing for the scaled wind turbine model are shown in Table 3. In the transition regions, the RBC PI control algorithm reduced the standard deviation of the rotor speed and generator power by 23.53% and 11.23%, respectively, compared with the baseline PI control algorithm. The DEL of the torsional load of the main shaft was reduced by 27.80%. In the rated power region, the RBC PI control algorithm reduced the standard deviation of the rotor speed and generator power by 29.91% and by 29.18%, respectively, compared with the baseline PI control algorithm.

Table 3. Quantitative comparison of control performance for scaled wind turbine model during wind tunnel testing.

Operating Region	Wind Tunnel Testing	Control Performance for Scaled Wind Turbine Model				
		Mean		Std. Dev.		DEL
		Ω_r (rpm)	P (W)	Ω_r (rpm)	P (W)	T (mNm)
Transition Region	Baseline PI (A)	680.333	39.765	19.539	1.398	2.171
	RBC PI (B)	681.669	39.643	14.942	1.241	1.567
	(B-A)/A (%)	0.196	−0.307	−23.527	−11.230	−27.803
Rated Power Region	Baseline PI (C)	677.813	39.722	24.186	1.436	0.000
	RBC PI (D)	681.690	39.753	16.953	1.017	0.000
	(D-C)/C (%)	0.572	0.078	−29.906	−29.178	0.000

Since the wind tunnel testing required the design of a controller for the scaled wind turbine model, the experiment using HILS was also performed for the scaled wind turbine model to compare the reasonable performance of the designed control algorithm. The normal operation of the scaled wind turbine model was simulated for 60 s under the conditions of average wind speeds of 6 m/s and 8 m/s, respectively, which are the transition and rated power regions. As with the NREL 5MW wind turbine, each simulation result

was analyzed to compare the performances of the baseline PI control algorithm and the RBC PI control algorithm for the scaled wind turbine model.

Figure 10 shows the results from the HILS testing of the baseline PI control algorithm and the RBC PI control algorithm for the scaled wind turbine model. Figure 10a shows the simulation results for transition regions, with an average wind speed of 6 m/s and a turbulent intensity of 10%. The transient responses in the transition regions can be seen at around 5 s, 32 s and 48 s in Figure 10a. As shown in Figure 9a, the results from the wind tunnel testing of the scaled wind turbine model showed that the RBC PI control algorithm responded appropriately to the transient responses in the transition regions by slowly using torque and pitch in advance. Sometimes, unlike the baseline PI control algorithm, the RBC PI control algorithm reduced the torque, but this was to regulate the biased reference generator speed. As a result, the deviations in rotor speed and generator power were reduced compared with the baseline PI control algorithm. Figure 10b shows the simulation results for the rated power region, with an average wind speed of 8 m/s and a turbulence intensity of 10%. Figure 10b shows, as with the wind tunnel testing results and the HILS testing results for the NREL 5MW wind turbine, that the two control algorithms maintained the generator torque at the rated value and performed pitch control to track the reference generator speed. As expected, the reference generator speed was biased using power feedback in the RBC PI control algorithm. Deviations in rotor speed and generator power were also reduced compared with the baseline PI control algorithm.

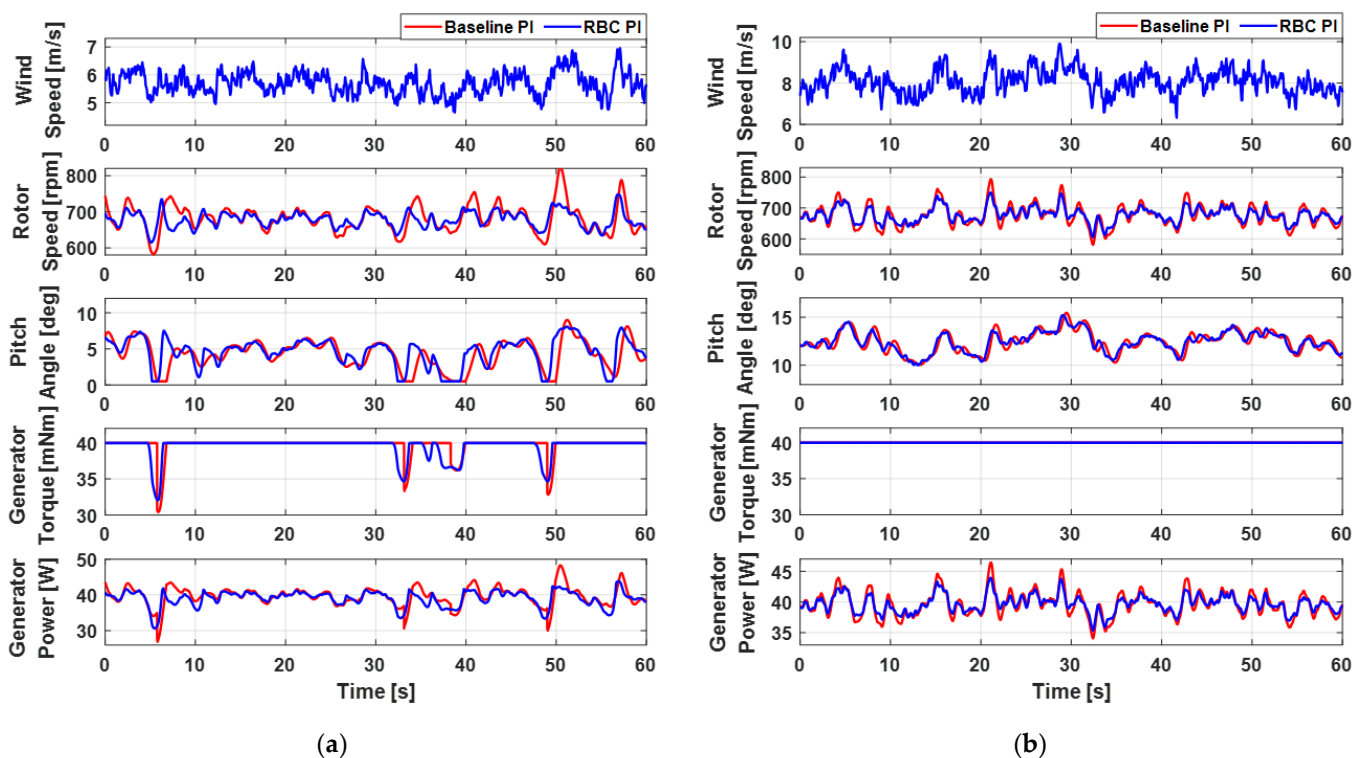


Figure 10. Results from HILS testing of scaled wind turbine model: (a) average wind speed of 6 m/s and 10% turbulence intensity; (b) average wind speed of 8 m/s and 10% turbulence intensity.

The results from the quantitative comparison of the simulations for the scaled wind turbine model are shown in Table 4. In the transition regions, the RBC PI control algorithm reduced the standard deviation of the rotor speed and generator power by 36.79% and 14.19%, respectively, compared with the baseline PI control algorithm. In addition, the RBC PI control algorithm improved the transient responses in the transition regions, thereby reducing the DEL of the torsional load of the main shaft by 35.78%. In the rated power region, the RBC PI control algorithm reduced the standard deviation of the rotor speed

and generator power by 30.04% and 29.69%, respectively, compared with the baseline PI control algorithm.

Table 4. Quantitative comparison of control performance for scaled wind turbine model during HILS testing.

Operating Region	HILS Testing	Control Performance for Scaled Wind Turbine Model				
		Mean		Std. Dev.		DEL
		Ω_r (rpm)	P (W)	Ω_r (rpm)	P (W)	T (mNm)
Transition Region	Baseline PI (A)	680.492	39.583	30.846	2.340	3.312
	RBC PI (B)	676.270	39.027	19.498	2.008	2.127
	(B-A)/A (%)	−0.620	−1.405	−36.789	−14.188	−35.779
Rated Power Region	Baseline PI (C)	677.152	39.663	34.164	2.001	0.000
	RBC PI (D)	677.307	39.665	23.900	1.407	0.000
	(D-C)/C (%)	0.023	0.005	−30.043	−29.685	0.000

The difference in the controller performances (Figures 7 and 10) for two wind turbines (NREL 5MW and Scaled model) are considered due to be the fact that the wind turbines and the wind conditions are different. The comparison results may vary to some extent depending on turbine specifications, such as the dynamic response of the pitch actuator, the dynamic characteristics of the generator, the material properties and the natural frequency of the tower, blade, etc. Therefore, it does not mean that the proposed RBC algorithm is more suitable for the scaled model compared with the large capacity wind turbines. It just means that the proposed RBC is effective for both wind turbines.

5. Discussion

In this section, the performance of the proposed RBC algorithm was compared with that of other Bias algorithms proposed in the literature [15,18].

Zalkind et al. applied a bias method similar to this study as a method for switching the blade pitch control strategy and the generator reaction torque control strategy in the transition region. However, the algorithms differ in the method and input variables for newly calculating the reference generator speed.

The RBC algorithm proposed in this study calculates the new reference generator speed of the blade pitch control loop and generator reaction torque control loop simultaneously and uses the blade pitch angle and generator power as input variables. The detailed structure of the RBC algorithm is shown in Figure 2. In the study by Zalkind et al., the set-point smoother (SPS) algorithm has the logic of determining whether the bias term is positive or negative so that the new reference generator speed is applied to only one of the two control loops (blade pitch control and generator reaction torque control) per each time step. In addition, the input variables for calculating the bias term are the blade pitch angle and the generator reaction torque as normalized single values. Figure 11 shows the block diagram of the SPS algorithm proposed by Zalkind et al.

HILS testing was performed in the transition region and the rated power region to compare the control performances of the RBC PI algorithm and the SPS PI algorithm. Figure 12 shows the HILS testing results. The normal operation of the NREL 5MW wind turbine was simulated for 200 s under conditions of average wind speeds of 13 m/s and 18 m/s, respectively. In order to compare and analyze the control performances of the two control algorithms, wind speed, rotor speed, blade pitch angle, generator torque, and generator power were obtained as shown in Figure 7. However, in consideration of the validity of the HILS testing results, Figure 12 used a different turbulence seed than Figure 7. Figure 12a shows the simulation results under conditions with an average wind speed of 13 m/s and a turbulence intensity of 19%, which is the transition region. In Figure 12a, the difference in control operations of the baseline PI, SPS PI, and RBC PI control algorithms

can be confirmed around 30 s to 150 s. The baseline PI control algorithm caused a sudden dip due to the use of switching logic. On the other hand, in the SPS PI and RBC PI control algorithm, it was found that the generator torque command was smoothed by the bias term. Figure 12b shows the simulation results under conditions with an average wind speed of 18 m/s and a turbulence intensity of 17%, which is the rated power region. In Figure 12b, it can be seen that the control performance of the baseline PI and the SPS PI control algorithm is almost similar. The reason is that the SPS algorithm performs only the smoothing function between the blade pitch and generator torque control strategy in the transition region of the bias term by blade pitch angle and generator reaction torque. Therefore, the control operations of the control algorithm of the baseline PI and the SPS PI in the rated power region are almost the same. On the other hand, since the RBC PI control algorithm includes a term for generator power in the bias term, it can be seen that the fluctuation of generator power and rotor speed is reduced compared with the control algorithm of baseline PI and SPS PI in the rated power region.

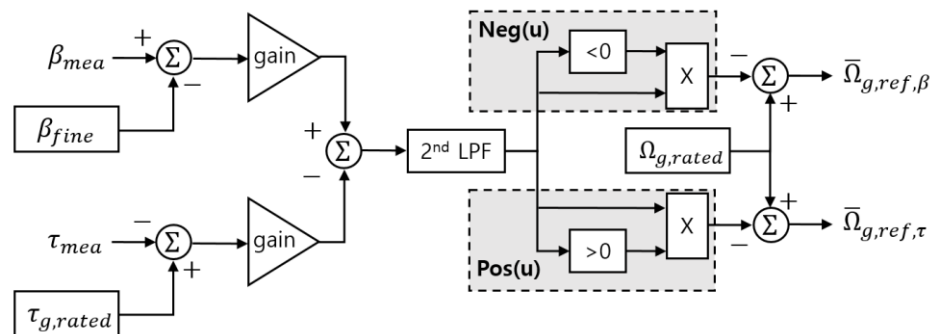


Figure 11. Block diagram of SPS algorithm for pitch and torque control loop.

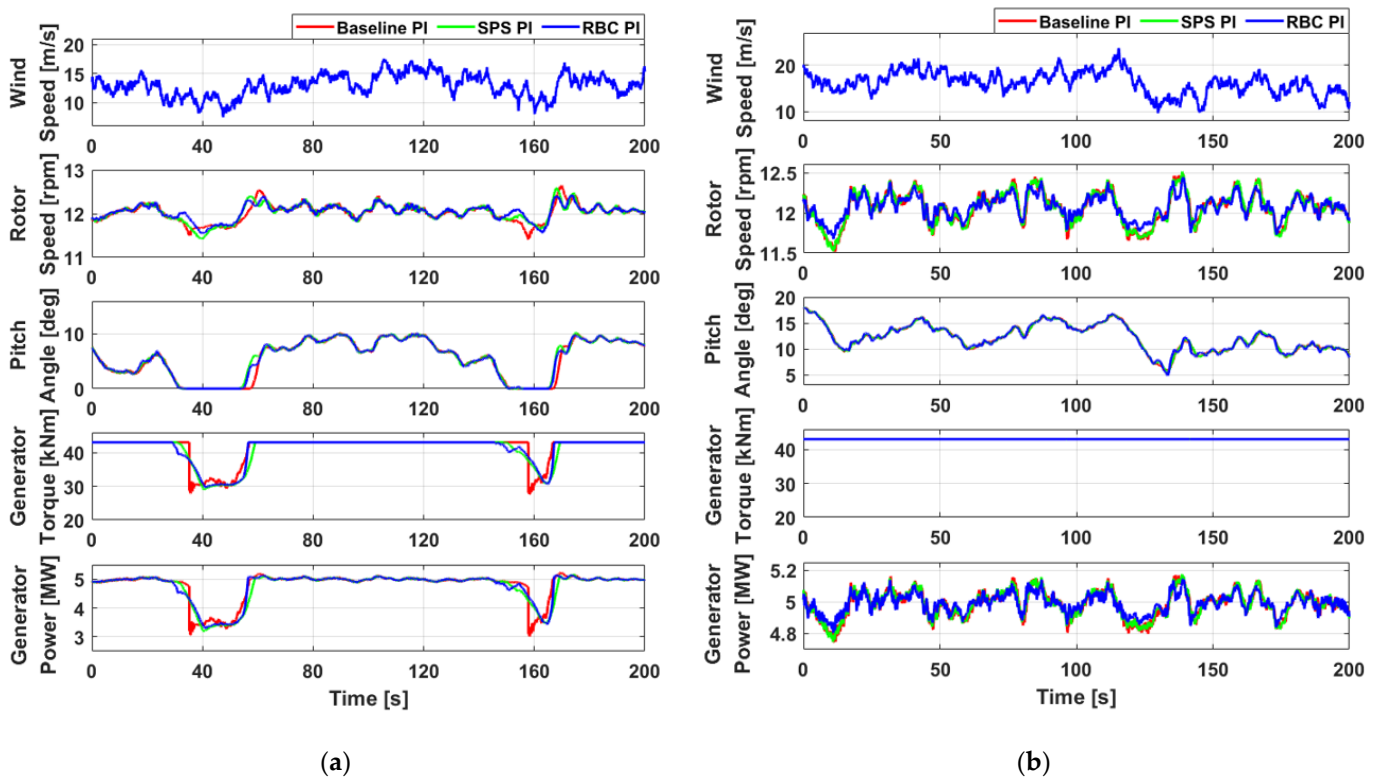


Figure 12. Results from HILS testing of NREL 5MW wind turbine for comparison of baseline PI, SPS PI, and RBC PI control performance: (a) average wind speed of 13 m/s and 19% turbulence intensity; (b) average wind speed of 18 m/s and 17% turbulence intensity.

The quantitative comparison results of HILS testing performed in Figure 12 are presented in Table 5. Both the SPS PI and RBC PI control algorithms in the transition region could reduce the fatigue load of the main shaft by about 20% compared with the baseline PI control algorithm by the smoothing function by the bias term. Furthermore, unlike the SPS PI control algorithm, the RBC PI control algorithm reduced the standard deviation of rotor speed and generator power by 15.85% and 4.49%, respectively. There was also a slight deviation reduction effect in the SPS PI control algorithm, but this effect was found to be due to the smoothing effect. In the rated power region, the SPS PI control algorithm did not improve the control performance by the bias term. As a result, there was no difference in the baseline PI control algorithm and control performance, which showed transient response only in the transition region, and the fatigue load of the main shaft was reduced by about 2.63%. On the other hand, the RBC PI control algorithm showed a reduction in the fatigue load of the main shaft by about 2.72% similar to the SPC PI control algorithm. In addition, the RBC PI control algorithm reduced the standard deviation of rotor speed and generator power by 26.25% and 25.48%, respectively, compared with the baseline PI control algorithm.

Table 5. Quantitative comparison of baseline PI, SPS PI, and RBC PI control performance for NREL 5MW wind turbine during HILS.

Operating Region	HILS Testing	Control Performance for NREL 5 MW Wind Turbine				
		Mean		Std. Dev.		DEL
		Ω_r (rpm)	P (MW)	Ω_r (rpm)	P (MW)	T (MNm)
Transition Region	Baseline PI (A)	12.024	4.785	0.201	0.511	1.231
	SPS PI (B)	12.595	4.753	0.195	0.510	0.989
	RBC PI (C)	12.430	4.774	0.169	0.488	0.987
	(B-A)/A [%]	4.750	−0.673	−2.972	−0.088	−19.645
	(C-A)/A [%]	3.373	−0.234	−15.851	−4.489	−19.817
Rated Power Region	Baseline PI (D)	12.071	4.988	0.195	0.082	1.138
	SPS PI (E)	12.072	4.988	0.195	0.081	1.108
	RBC PI (F)	12.078	4.991	0.144	0.061	1.107
	(E-D)/D [%]	0.010	0.010	0.361	−0.093	−2.634
	(F-D)/D [%]	0.060	0.059	−26.248	−25.477	−2.722

6. Conclusions

In this study, an RBC PI controller with an RBC algorithm was designed to further improve control performance while maintaining the structure of a conventional control algorithm. The wind turbine model that was used in this study was the NREL 5MW wind turbine and HILS testing using commercial PLC and aero-elastic analysis programs were performed to compare the performances of a conventional baseline PI control algorithm and the proposed RBC PI control algorithm.

From the HILS testing, we found that the RBC PI control algorithm was effective in improving the transient responses that occurred in the transition regions. Deviations in rotor speed and generator power and the DEL of the main shaft were reduced. Due to the influence of the biased reference generator speed, deviations in rotor speed and generator power even decreased in the rated power region. Quantitatively, deviations in rotor speed and generator power were reduced by 22.40% and 21.35%, respectively, and the torsional DEL was reduced by 14.74%. Wind tunnel testing was conducted using a scaled wind turbine model to experimentally validate the performance of the RBC PI control algorithm, which was confirmed by the HILS testing.

From the wind tunnel testing, we found that the RBC PI control algorithm, as in the HILS testing, improved the sudden dips, which are transient responses that occur in transition regions. The blade pitch angle and generator torque were used in the RBC PI

control algorithm before the baseline PI control algorithm, thereby reducing fluctuations in the rotor speed and generator power and the torsional DEL of the main shaft by 23.53%, 11.23% and 27.80%, respectively. In the rated power region, deviations in rotor speed and generator power were reduced by 30.04% and 29.69%, respectively.

In conclusion, the RBC PI control algorithm proposed in this paper could improve the sudden dip in generator torque and power without completely replacing the conventional structure with other structures and reduce the fluctuation of the main shaft load and power. As a result, the power quality is improved and the fatigue load of the wind turbine is reduced such that the failure of the wind turbine may be reduced through the stable operation of the wind turbine. However, the proposed algorithm has not been validated with actual large-scale wind turbines through field tests, and therefore further experimental validations will be necessary before the algorithm can be applied to commercial large-scale wind turbines to improve power performance.

Author Contributions: Conceptualization, T.J. and D.K.; methodology, T.J.; software, T.J.; supervision, I.P.; validation, T.J. and D.K.; writing—original draft preparation, T.J.; writing—review and editing, I.P. All authors have read and agreed to the published version of the manuscript.

Funding: This work was supported by the Energy Efficiency and Resources Program and the New and Renewable Energy-Core Technology Program of the Korea Institute of Energy Technology Evaluation and Planning (KETEP), with granted financial resources from the Ministry of Trade, Industry and Energy, Republic of Korea (grants numbers 20204030200010 and 20203030020270).

Institutional Review Board Statement: Not applicable.

Informed Consent Statement: Not applicable.

Data Availability Statement: Not applicable.

Conflicts of Interest: The authors declare no conflict of interest.

Nomenclature

Symbols

$\Omega_{g,ref,dppt}$	Reference generator speed for DPPT control
$\Omega_{g,rated}$	Rated generator speed
P_{cmd}	Power command
$k_{g,opt}$	Optimal torque gain at generator
P_{mea}	Measured power
P_{rated}	Rated power
$\delta\xi_{\beta}$	Reference bias at pitch control
$\delta\xi_{\tau}$	Reference bias at torque control
$\bar{\Omega}_{g,ref}$	Reference generator speed
$\tau_{g,ref,dppt}$	Reference generator torque for DPPT control
$\tau_{g,rated}$	Rated generator torque
$\tau_{UL,dppt}$	Upper limit of generator torque for DPPT control
$\Omega_{g,mea}$	Measured generator speed
τ_{LL}	Lower limit of generator torque
$\tau_{LL,dppt}$	Lower limit of generator torque for DPPT control
k_p	Proportional gain
k_i	Integral gain

References

1. Manwell, J.F.; Mcgowan, J.G.; Rogers, A.L. *Wind Energy Explained*, 2nd ed.; John Wiley & Sons Ltd.: Hoboken, NJ, USA, 2009.
2. Bossanyi, E.A. The design of closed loop controllers for wind turbines. *Wind Energy* **2000**, *3*, 149–163. [[CrossRef](#)]
3. Nam, Y. *Wind Turbine System Control*, 1st ed.; GS Interscience: Seoul, Korea, 2013.
4. Bianchi, F.; De Battista, H.; Mantz, R. *Wind Turbine Control Systems: Principles, Modelling and Gain Scheduling Design*; Springer Verlag: London, UK, 2007.

5. Nam, Y.; Kim, J.; Paek, I.; Mun, Y.; Kim, S.; Kim, D. Feedforward pitch control using wind speed estimation. *J. Power Electron.* **2011**, *11*, 211–217. [[CrossRef](#)]
6. Dixit, A.; Suryanarayanan, S. Towards pitch-scheduled drive train damping in variable-speed, horizontal-axis large wind turbines. In Proceedings of the 44th IEEE Conference on Decision and Control, Seville, Spain, 12–15 December 2005; pp. 1295–1300.
7. Kim, K.; Kim, H.-G.; Paek, I. Application and Validation of Peak Shaving to Improve Performance of a 100 KW Wind Turbine. *Int. J. Precis. Eng. Manuf. Green Tech.* **2020**, *7*, 411–421. [[CrossRef](#)]
8. Bossanyi, E.A. Wind turbine control for load reduction. *Wind Energy* **2003**, *6*, 229–244. [[CrossRef](#)]
9. Pham, T.; Nam, Y.; Kim, H.; Son, J. LQR control for a multi-MW wind turbine. *World Acad. Sci. Eng. Technol.* **2012**, *62*, 670–675.
10. Jeon, T.; Paek, I. Design and Verification of the LQR Controller Based on Fuzzy Logic for Large Wind Turbine. *Energies* **2021**, *14*, 230. [[CrossRef](#)]
11. Jeon, T.; Kim, D.; Song, Y.; Paek, I. Design and Validation of Demanded Power Point Tracking Control Algorithm for MIMO C-controllers in Wind Turbines. *Energies* **2021**, *14*, 5818. [[CrossRef](#)]
12. Barcena, R.; Acosta, T.; Etxebarria, A.; Kortabarria, I. Wind Turbine Structural Load Reduction by Linear Single Model Predictive Control. *IEEE Access* **2020**, *8*, 98395–98409. [[CrossRef](#)]
13. de Corcuera, A.D.; Pujana-Arrese, A.; Ezquerro, J.M.; Seguro, E.; Landaluze, J. H ∞ Based Control for Load Mitigation in Wind Turbines. *Energies* **2012**, *5*, 938–967. [[CrossRef](#)]
14. Ruz, M.L.; Garrido, J.; Fragos, S.; Vazquez, F. Improvement of Small Wind turbine Control in the Transition Region. *Energies* **2020**, *8*, 244. [[CrossRef](#)]
15. Zalkind, D.S.; Nicotra, M.M.; Pao, L.Y. Constrained power reference control for wind turbines. *Wind Energy* **2022**, *25*, 914–934. [[CrossRef](#)]
16. Pao, L.; Johnson, K. A Tutorial on the Dynamics and Control of Wind turbines and Wind Farms. In Proceedings of the American Control Conference, Boulder, CO, USA, 10–12 June 2009; pp. 2076–2089.
17. Kim, K.; Kim, H.-G.; Song, Y.; Paek, I. Design and Simulation of an LQR-PI Control Algorithm for Medium Wind Turbine. *Energies* **2019**, *12*, 2248. [[CrossRef](#)]
18. Abbas, N.J.; Zalkind, D.S.; Pao, L.; Wright, A. A reference open-source controller for fixed and floating offshore wind turbines. *Wind Energy Sci.* **2022**, *7*, 53–73. [[CrossRef](#)]
19. Zalkind, D.S.; Pao, L.Y. Constrained for wind turbine power control. In Proceedings of the American Control Conference, Philadelphia, PA, USA, 10–12 July 2019; pp. 3494–3499.
20. Jonkman, J.; Butterfield, S.; Musial, W.; Scott, G. *Definition of a 5-MW Reference Wind Turbine for Offshore System Development*; NREL/TP-500-38060; National Renewable Energy Lab. (NREL): Golden, CO, USA, 2009.
21. DNV. *Bladed Hardware Test Module User Manual*; Version 3.0; Garrad Hassan & Partners Ltd.: Bristol, UK, 2021.
22. International Electrotechnical Commission. *IEC 61400-1 Wind Energy Generation Systems—Part 1: Design Requirements*, 4th ed.; International Electrotechnical Commission: Geneva, Switzerland, 2019.
23. Campagnolo, F.; Petrovic, V.; Nanos, E.M.; Tan, C.W.; Bottasso, C.L.; Paek, I.; Kim, H.; Kim, K. Wind tunnel testing of power maximization control strategies applied to a multi-turbine floating wind power platform. In Proceedings of the 26th International Ocean and Polar Engineering Conference, ISOPE-I-16-307, Rhodes, Greece, 26 June–1 July 2016.